Supplementary material:

Supplementary Text 1: Supplementary materials and methods

Supplementary Text 2: Histopathological changes in *Toxoplasma gondii* infected dunnarts at 7 and 14 days p.i. and *Neospora caninum* infected dunnarts at 7 and 13 days p.i.

Supplementary Figure 1: Daily activity and food consumption of fat-tailed dunnarts (*Sminthopsis crassicaudata*) during *Neospora caninum* and *Toxoplasma gondii* infection. Data shown are representative of two independent *T. gondii* experiments (Tg1: A, E, I; Tg2: B, F, J) and two independent *N. caninum* experiments (Nc1: C, G, K; Nc2: D, H, L). Activity and food consumption of all experimental animals was individually monitored and is presented as a daily sum. Daily activity was measured on an exercise wheel equipped with a wheel odometer that translated the number of revolutions in 24 hours into distance in kilometers (C, D, I, J) and time spent in the wheel (A, B, G, H). Food consumption reflects the total grams of food consumed in 24 hours (E, F, K, L). Uninfected control animals are designated by a red line connecting data points.

Supplementary Table 1: Summary of parasite infection experiments in the fat-tailed dunnart (*Sminthopsis crassicaudata*)

Supplementary Table 2: Oligonucleotide primer sequences used in qPCR in the present study

Supplementary Table 3: Optimization values for qPCR assays used in the present study

Supplementary Table 4: Summary of histopathology lesion grading scores for inflammation, necrosis, and parasite life stage in *Neospora caninum* and *Toxoplasma gondii* infected fat-tailed dunnarts (*Sminthopsis crassicaudata*)

Supplementary Table 5. Summary of parasite tissue load in the brain, tongue, lung, heart, liver, and spleen of fat-tailed dunnarts (*Sminthopsis crassicaudata*) at 7 and 13-14 days postinfection with *Toxoplasma gondii* and *Neospora caninum*. Parasite numbers represent group median values (interquartile range) based on four biological replicates. Data shown are representative of two independent *T. gondii* experiments and two independent *N. caninum* experiments. Abbreviation: p.i., postinfection.

Supplementary Table 6. Summary of cytokine mRNA expression (fold change) in fat-tailed dunnarts (*Sminthopsis crassicaudata*) experimentally infected with *Toxoplasma gondii* and *Neospora caninum* at 7 and 13-14 days p.i., determined by qRT-PCR. Cytokine mRNA expression has been normalized to the geometric mean of GAPDH and 28S. Data reflect group median values (interquartile ranges) based on four biological replicates. Data shown are representative of two independent *T. gondii* experiments and two independent *N. caninum* experiments. Control, uninfected dunnarts; p.i., postinfection

SUPPLEMENTARY TEXT S1 Supplementary Materials and Methods

Animal housing. Animals were housed individually in a temperature controlled environment (20-22°C) with a 12h light:12 hour dark photocycle, and received fresh water and mixed cat food (1:2 ratio of moistened Optimum® Furball biscuits: canned Whiskas® Loaf Lamb with Kidney) *ad libitum*.

Preparation of *N. caninum* and *T. gondii* tachyzoites for parasite infection and immunological studies. Tachyzoites of NC-Nowra isolate of *Neospora caninum* and TgAuDg1 isolate of *Toxoplasma gondii* were propagated *in vitro* by serial passages at the University of Sydney (up to 5 and 13 passages for TgAuDg1 and NC-Nowra, respectively) in African green monkey kidney adherent fibroblast (Vero cell) cultures under the following conditions. Parasite cultures were maintained in a humidified incubator at 5% CO_2 and 37°C using Dulbecco's Modified Eagle's Medium High Glucose (DMEM-HG) (Sigma-Aldrich, Australia) supplemented with 2% heat-inactivated fetal bovine serum (GIBCO™, ThermoFisher Scientific, Australia) and 1% penicillin-streptomycin antibiotics (GIBCO™, ThermoFisher Scientific, Australia). Prior to inocula preparation, parasite cultures were tested for mycoplasma contamination using the Venor®GeM OneStep *Mycoplasma* Detection Kit for endpoint PCR (Minerva Biolabs, Biocene, Australia) as per manufacturer's instructions. For inocula preparation, infected Vero cells were cultured until cytopathic effects were observed in 40-60% of the host cell monolayer and remaining cells were heavily infected. A cell scraper was used to harvest adherent infected cells and the supernatant containing free and intracellular

tachyzoites was passed through a 26½ gauge needle five times to liberate intracellular parasites. Tachyzoites were then purified by passage through a sterile 5-µm nitrocellulose membrane filter (Millipore Corporation, Bedford, MA USA), stained with 0.4% Trypan Blue Solution (GIBCO™, ThermoFischer Scientific, Australia) to assess viability, counted with a hemocytometer and suspended in sterile phosphate-buffered solution (PBS) to achieve a concentration of 3.33×10^5 viable tachyzoites/ml. Tachyzoites of NC Nowra isolate of *Neospora caninum* and TgAuDg1 isolate of *Toxoplasma gondii* are cryopreserved at the University of Technology Sydney (Sydney, Australia).

Tissue sampling and storage. Animals were necropsied immediately after euthanasia. Heart blood was collected and allowed to clot before centrifugation at 1,000 x g for 15 min; serum was removed and stored at -20°C until serological analysis. Sterile samples of brain, lung, heart, liver, spleen, and skeletal muscle were collected in cryovials, and either flash frozen in liquid nitrogen before storage at -80°C or placed directly into a -80°C freezer immediately after collection until RNA and DNA isolation. Frozen spleen samples were later transferred to new tubes containing 1.0 ml RNAlater (Applied Biosystems, Carlsbad, CA, USA) to stabilize nucleic acids for long term storage, stored at -4°C overnight and then -20°C after a pilot study determined thawing spleen in RNAlater had no detrimental effect on subsequent RNA and DNA synthesis. Samples of brain, eye, tongue, nasal cavity, salivary gland, thyroid gland, esophagus, trachea, heart, diaphragm, multiple lymph nodes, usually including thoracic and mediastinal, mesentery, stomach, duodenum, jejunum, ileum, pancreas, spleen, liver, gall bladder,

kidney, ureter, adrenal gland, urinary bladder, reproductive structures (either uterus and ovary or testicle, epididymis, and prostate gland), forelimb skeletal muscle, elbow joint, peripheral nerve, bone marrow, and bone were collected and placed in 10% neutral buffered formalin (pH 7.0) for histopathological assessment. Tissue samples containing bone were decalcified for 24-28h prior to processing for histopathology.

Clinical evaluation of *N. caninum* and *T. gondii* infection. To assess animal activity throughout the experiment, animals were monitored using a 24h surveillance system with infrared capacity to record animal movements. Video footage was reviewed twice daily to evaluate for clinical manifestations of disease. Additionally, each cage contained a rodent exercise wheel equipped with an odometer that recorded running time and distance travelled over a 24h period. Food and water intake were measured daily. Body mass (g) and tail base width (mm, an indicator of general health for this species) were monitored throughout the experiment. Data was recorded for each animal for 6-7 days prior to inoculation in order to obtain a baseline of individual activity and food consumption. Animals presenting with signs of clinical disease, including excessive water consumption, decreased appetite and activity, ungroomed pelage, hunched body posture, and abnormal behavior were removed from their cage and weighed. The following humane end-points were used to determine the conclusion of the experiment: 20% loss of original body weight, severe dehydration, labored respiration, neurological clinical signs, obtunded behavior, and urinary incontinence. Animals found to be meeting any of these criteria were immediately euthanized by CO_2 inhalation. Morbidity

scores were assigned to each animal to facilitate statistical analysis as previously described (1).

Pathological analysis. A complete postmortem exam was performed on each animal and included assessment of overall body condition, external examination, evaluation of subcutaneous and visceral adipose tissue stores and skeletal musculature, and macroscopic examination of thoracic and abdominal organs. Body mass, tail base measurements, and total spleen weight were recorded.

Formalin-fixed and decalcified tissues were processed routinely, embedded in paraffin wax, and 4-µm thick sections were stained with hematoxylin and eosin (H&E) and evaluated by light microscopy. Results for histopathological analysis of brain, tongue, lung, heart, liver, and spleen were expressed by score criteria based on a semiquantitative analysis that evaluated the severity of inflammation and necrosis, and presence of different parasite life stages. For the evaluated sectional area of a given tissue, the extent of inflammation and necrosis were scored separately and scoring ranged from no lesion present (score = 0) to minimal (<5% affected; score = 1), mild (5-10% affected; score = 2), moderate (11-30% affected; score = 3), or severe (>30% affected; score = 4). To evaluate for the presence of different parasite life stages, scoring ranged from none present (score = 0) to tachyzoites only (score = 1), tissue cysts only (score = 2), or tachyzoites and tissue cysts (score = 3). Criteria were established in order to distinguish between true tissue cysts and pseudocysts; a tissue cyst was defined as a discrete intracellular accumulation of zoites not directly associated with inflammatory infiltrates or necrosis. Tissue cysts identified in H&E

sections were confirmed using bradyzoite specific BAG5 IHC. Histopathology was assessed without prior knowledge of the origin of each tissue. The final histopathology grading scores for inflammation and necrosis used for data analysis were based on the averaged scores assigned by two pathologists, including a board-certified veterinary pathologist. Lesion severity scores for each tissue are based on the sum of the necrosis and inflammation score.

Immunohistochemistry (IHC) was performed on paraffin embedded tissue sections using rabbit anti-*Toxoplasma gondii* polyclonal serum (RB-282-A1, Thermo Fischer Scientific, Fremont, CA, USA) and goat anti-*Neospora caninum* polyclonal serum (210-70-NC, VMRD, Pullman, WA, USA) at a 1:000 and 1:6000 dilutions respectively using methods described previously (2, 3) with the inclusion of a 20 min protein blocking step (CANDOR Bioscience GmbH, Wangen, Germany) for *N. caninum* to diminish nonspecific background staining. Positive controls included feline spinal cord (*T. gondii*) and fetal white rhinoceros liver (*N. caninum*) containing parasites. To detect *T. gondii* and *N. caninum* bradyzoites, the polyclonal rabbit antibody anti-TgBAG5 was used at a 1:300 dilution as previously described (2) with the inclusion of a 20 min protein blocking step to reduce nonspecific staining. For negative controls, IHC techniques were applied with omission of the primary antiserum.

Quantification of tissue parasite load from *N. caninum* and *T. gondii* infected dunnarts. For each experimental animal, genomic DNA was extracted from 25mg of brain (frontal lobe), tongue, lung, heart, liver, and spleen using the Isolate II Genomic DNA kit (Bioline, Australia) using the recommended manufacturer's protocol for

purifying DNA from animal tissue. As a negative DNA extraction control, 25 µl of sterile distilled water was processed along with all samples. DNA samples were eluted in 100 µl Elution Buffer G with the exception of brain which was eluted in a volume of 60 µl. DNA was quantified and checked for purity using a NanoDrop ND-1000 Spectrophotometer (ThermoFisher Scientific, Australia), diluted with PCR grade water to achieve a final concentration of 20 ng/µl, and separated into single use aliquots prior to storage at -20°C until use. To generate standard curves for parasite quantification and for use as a positive control, genomic DNA was extracted from known numbers of *N. caninum* and *T. gondii* tachyzoites using the Isolate II Genomic DNA kit following manufacturer's protocol.

Parasite tissue burden was assessed by quantitative PCR (qPCR) in SYBR Green based assays targeting the *T. gondii* SAG1 gene (4) and *N. caninum* Nc5 gene (5) (see Tables S2 and S3 for primer sequences and assay optimization conditions). All samples were tested in triplicate qPCR reactions containing 10 µl of SsoAdvanced universal SYBR® Green supermix, either 0.4 µl of each SAG1 primer (20µM) or 1.0 µl of each Nc5 primer (20µM), 5 µl DNA template (100ng DNA), and PCR grade water to achieve a final volume of 20 µl. Amplification and data acquisition were carried out in the CFX96 Touch™ Real-Time PCR Detection System with the corresponding CFX 108 Manager 3.1 software (BioRad, Australia). Amplification cycling conditions were 95°C for 10 min (activation) followed by 40 cycles of 95°C for 15 s (denaturation) and 60°C for 60 s (annealing and extension). Each run included no-template negative controls, inter-run calibrators to control for inter-run variation, and a standard curve generated using 10-fold serial dilutions (equivalent of 3 to 3 X 10^5 *T. gondii* parasites or 6 to 6 X 10^5 *N.*

caninum parasites). A melting curve analysis was acquired for PCR products after completion of cycling conditions by a pre-melt conditioning step at 55°C for 90 s followed by stepwise 1 s incremental temperature increases of 1°C from 55°C to 95°C. Melt curves were visually assessed for all PCR products to confirm the identity of the desired product and amplification products were randomly selected to confirm amplicon length using a 1.5% agarose gel stained with GelRed (Biotium, Australia). Calculation of quantification cycle (Cq) was based on automatic software analysis single baseline setting parameters. Samples were considered positive if at least 2 of 3 replicates had a Cq < 36. Any sample with a Cq ≥ 36 was considered negative. Samples with only 1 of 3 replicates registering a Cq < 36 were analyzed again for confirmation and deemed positive if the same conclusion was reached in the second run. Data handling and calculations for qPCR data were carried out in qBase^{PLUS} Version 3.0 (Biogazelle, Ghent, Belgium). Raw Cq values were exported to Microsoft excel and uploaded to qBase^{PLUS} where run specific PCR efficiency E was calculated from the standard curve slope using linear regression and inter-run calibration (IRC) was performed using inter-run calibrators to correct for inter-run variation prior to analysis (6). Parasites were quantified in different tissue samples using the average Cq values for each sample by interpolation of standards of known quantity included with each run to obtain the calibrated normalized relative quantity (CNRQ) of parasites present in each sample and expressed as $\log_{10}$ parasites per 100ng of total DNA. The limit of detection for *N. caninum* and *T. gondii* were < 1 parasite and 2 parasites in 100ng DNA, respectively.

Mitogen stimulation of dunnart splenocytes. The spleen was aseptically collected from an uninfected control dunnart at necropsy. Single-cell suspensions of spleen cells (splenocytes) were obtained by gentle tissue extrusion through a 70 µm cell strainer in the presence of DMEM-HG (Sigma-Aldrich, Australia). Suspended cells were centrifuged at 800 x g for 5 min, the supernatant aspirated, and cells resuspended in DMEM and centrifuged again at 800 x g for 5 min. After centrifugation and removal of supernatant, the cells were resuspended at 1 x 10^6 nucleated cells/ml with DMEM-HG supplemented with 10% FBS (GIBCO™, ThermoFischer Scientific, Australia), 50 ng/ml Phorbol myristate acetate (PMA) (Sigma-Aldrich, Australia), and 1 µg/ml Ionomycin (Sigma-Aldrich, Australia). 1 ml volumes of splenocyte suspensions were incubated in sealed tubes at 37°C, and 5% CO_2 for 7 h (7, 8). After incubation, splenocytes were pelleted by centrifugation (900g x 5m), washed twice with warm sterile PBS, resuspended in RNAlater (Applied Biosystems, Carlsbad, CA, USA), stored overnight at -4°C and then -20°C for later RNA extraction.

Transcriptome generation and analysis. With the goal of identifying dunnart immune transcripts for qPCR assay design, four separate transcriptomes were generated using total RNA isolated from the following samples: (1) 1 x 10^6 mitogen-stimulated splenocytes from an uninfected dunnart (JS2093), (2) spleen from an uninfected dunnart (JS1633), (3) spleen from a *N. caninum* infected dunnart at 2 weeks p.i. (JS2095), and (4) spleen from a *T. gondii* infected dunnart at 2 weeks p.i. (JS2097). For RNA extraction from mitogen-stimulated splenocytes stored in RNAlater, samples were centrifuged for 2300 x g for 15m and RNAlater aspirated from the cell pellet. Cells

were homogenized by the direct addition of Lysis Buffer RLY and RNA was isolated using the ISOLATE II RNA Mini Kit (Bioline, Australia) including an on-column DNAse I treatment (supplied in the kit) as per manufacturer's protocol. For RNA extraction from dunnart spleens, 20 mg of tissue was placed in 2 ml FastPrep® Lysis Bead Matrix D tubes (MP Biomedicals, LLC, Australia) containing 600 µl Lysis Buffer RLY from the ISOLATE II RNA Mini Kit and 6µl of β-ME and homogenization was achieved using a FastPrep®-24 Instrument (MP Biomedicals, USA) for 30 s at 6 m/s. Following homogenization, samples were centrifuged at 12,000 x g for 5 min and the upper phase of the lysate was removed and transferred to the ISOLATE II filter from the ISOLATE II RNA Mini Kit. Remaining RNA isolation including on-column DNAse I treatment of RNA was done using the ISOLATE II RNA Mini Kit following manufacturer's protocol. RNA samples were eluted in 50 µl RNase-free water. RNA concentration and purity were determined using a NanoDrop ND-1000 Spectrophotometer (ThermoFisher Scientific, Australia) and RNA integrity was assessed by chip-based micro-electrophoresis using an Agilent 2100 Bioanalyzer (Agilent Technologies, Waldbronn, Germany). RNA samples were transferred into tubes containing RNAstable® (Biometrica) and allowed to dry for 1.5 hours at ambient temperature using a Savant SpeedVac® (ThermoFisher Scientific, Australia) according to manufacturer's instructions. Illumina HiSeq2000 RNA sequencing was carried out at Macrogen (Seoul, Korea). Four libraries were generated and a total of 48.3 – 74.4 million raw sequence reads obtained per library.

Read quality was assessed with FastQC using the default parameters before assembly with Trinity v2.3.2 (9) and filtering for 'good transcripts' with Transrate v1.0.3 (doi:10.1101/gr.196469.115), both using the default parameters. Raw sequence reads

from each database were submitted to NCBI SRA under the Bioproject PRJNA356957. This Transcriptome Shotgun Assembly project has been deposited at DDBJ/EMBL/GenBank under the accession GFCN00000000. The version described in this paper is the first version, GFCN01000000. We used Salmon v0.7.2 (https://combine-lab.github.io/salmon) to quantify transcripts in each library and calculate the weighted trimmed mean of the log expression (M) ratios [trimmed mean of M values (TMM)] (10) for cytokines listed in Table 1, which we identified as the reciprocal best BLAST hits of orthologs in any marsupial for which sequence was available, or from human orthologs.

Design and validation of qRT-PCR assays to evaluate cytokine expression. Cytokine transcript sequences for IFN-γ, TNF-α, IL-4, IL-17A, and IL-6 obtained from the dunnart spleen transcriptome were checked for secondary structures using UNAFold (http://sg.idtdna.com/UNAFold) and if present, regions of high secondary structure were avoided when designing primers. Primers were designed using Primer3Plus (11) and recommended parameters for designing SYBR® Green primers (12). Primer sequences were evaluated for interactions, secondary structures, and specificity against nonspecific marsupial sequences using BeaconDesigner™ Free Edition Software (http://www.premierbiosoft.com/qOligo/Oligo.jsp?PID=1) and NCBI Primer-BLAST (13). All assays were designed within exons and amplicon length varied between 91 and 178 base pairs long. Oligonucleotide primers were synthesized by Macrogen (Korea). Optimal annealing temperatures were determined by gradient PCR analysis and primers were titrated as needed to diminish primer-dimer formation in no

template controls. Amplicon specificity was checked by melt curve analysis, visualization of a single amplicon on an agarose gel stained with GelRed (Biotium, Australia), and confirmed by bi-directional sequencing (Macrogen, Korea). Primer sequences used for 28S and GAPDH reference gene amplification were obtained from the literature (8, 14) and aligned with dunnart 28S and GAPDH gene sequences to ensure 100% nucleotide identity using CLC Main Workbench v6.9 (CLCbio, Denmark). qPCR assays were carried out in the CFX96 Touch™ Real-Time PCR Detection System (Bio-Rad Laboratories Inc., CA, USA. Triplicate technical replicates were run for each sample in a final volume of 20 µl with 10 µl of SsoAdvanced universal SYBR® Green supermix, 1 µl of each primer, 2 µl of cDNA template (1:10 dilution), and 6 µl of PCR grade water. Cycling conditions included an initial activation step of 95°C for 10m followed by 40 cycles of denaturation for 15s at 95°C and annealing/extension for 60s at 60°C (57°C for GAPDH and IL-6). Upon completion of PCR cycling, PCR amplification products were subjected to a melting curve analysis to assess reaction specificity and confirm identity by verifying specific melting temperature (T_m) profiles. The melting curve analysis was carried out at 52°C to 95°C by increasing the temperature by 1.0°C/1s following a pre-melt conditioning step at 55°C for 90s. Each run included no template negative controls and no-RT controls.

To determine each assay's reaction efficiency, dynamic range, limits of quantification (LOQ) and detection (LOD), y-intercept, slope, and r^2 calibration curve, standard curves were established for each cytokine using 10-fold serial dilutions prepared from purified PCR product quantified by a NanoDrop ND-1000 spectrophotometer (ThermoFisher Scientific, Australia). PCR products were diluted until

the standard curve was no longer linear (LOQ) and amplification was no longer detected (LOD). Efficiency was calculated using the formula $10^{(-1/slope)} - 1$. DNA molecule copy number was calculated from DNA concentration using the following formula: copy number = [ng DNA x 6.022 x 10^{23}]/[amplicon length (bps) x 10^{9} ng g^{-1} x 660 g mol^{-1} bps^{-1}].

Splenic cytokine mRNA expression by qPCR. Total RNA was prepared from the spleens of experimental dunnarts using the Isolate II RNA Mini Kit and homogenization and extraction techniques and on-column DNase treatment as previously described for transcriptome generation. RNA samples were stored at -80°C until cDNA synthesis. RNA quantity and quality were evaluated by spectrophotometry and Agilent 2100 expert chip system and RNA extraction was repeated for any sample with RIN < 7.5. RNA samples were subjected to an additional DNase treatment using the TURBO DNA-*free*™ Kit (ThermoFisher Scientific, Australia) as per manufacturer's instructions immediately prior to reverse transcription to eliminate or reduce remaining genomic DNA contamination to negligible levels. cDNA was synthesized from 2 µg total RNA in a final volume of 20 µl using the Revertaid First Strand cDNA Synthesis Kit (ThermoFisher Scientific, Australia) using a 50:50 mixture of random hexamer and oligo$(dT)_{18}$ primers (1 µl each), following the protocol for oligo$(dT)_{18}$ synthesis with inclusion of an initial RNA-primer incubation step at 65°C for 5m to denature RNA prior to reverse-transcription. Control (no-RT) reactions omitting reverse transcriptase were prepared at the same time to evaluate RNA samples for genomic DNA (gDNA) contamination. cDNA synthesis reactions were carried out in a Veriti® Thermal Cycler

(ThermoFisher Scientific, Australia). Upon completion of reverse transcription, cDNA and no-RT controls were diluted 1:10 with RNase/DNase-free water and evaluated by 28S qPCR to assess for gDNA contamination and efficiency of cDNA synthesis. After evidencing negligible gDNA contamination of samples (i.e., less than 0.1% gDNA present in RNA) by demonstrating a difference of >10 cycle thresholds between no-RT and RT+ samples, cDNA was separated into single-use aliquots and stored at -20°C until cytokine evaluation. To investigate relative cytokine expression for IFN-γ, TNF-α, IL-4, IL-17A, and IL-6, qPCR reactions targeting these genes and target reference genes were carried out in triplicate reactions for each sample using methods described above. 28S and GAPDH were used as reference genes to normalize the results for each sample to correct for variations in input RNA due to degradation, extraction efficiency, and reverse transcription. All samples for a given gene were analyzed in a single run (sample maximization strategy) to eliminate the need for inter-run calibration. Raw Cq scores, determined by baseline settings in the CFX 108 Manager 3.1 software (BioRad, Australia), were uploaded to qBase^{PLUS} software where the geometric mean of GAPDH and 28S was used to normalize expression level of each target transcript in each sample and ‘target specific amplification efficiency’ and ‘scale to control’ parameters were selected to generate CNRQ value of cytokine expression for each sample (6). The reference genes GAPDH and 28S have been previously validated for use in koalas and tammar wallabies and were evaluated for suitability of use in parasite-infected dunnarts in this study by calculating reference gene stability between treatment groups using the qBase^{PLUS} software (8, 14). The mean geNorm M-value and coefficient of variation for GAPDH and 28S were found to be equal to 0.734 and 0.257

respectively, evidencing their suitability for use as reference genes (M-values <1 and CV < 0.5 are recommended for reference genes) (6). The assays designed for this assay were sensitive, reproducible, and all samples tested fell within the linear dynamic range for all genes assayed with the exception of IL-17A for which several samples failed to produce a minimum amount of signal to generate a Cq value in all three triplicate samples (non-detects). Non-detects were handled by setting undetermined values to the median of the detected replicates or to a maximum Cq value (40) if the majority were non-detects (15) which equated to less than 1 transcript copy for fold difference calculations in order to facilitate inclusion of these samples for statistical analysis. Technical error and RNA degradation were unlikely to have contributed to failed amplification in these cases because IL-17A mRNA amplification occurred in other samples included in the same run and RNA quality was high when assessed using recommended MIQE guidelines (16)

References

1. **Bartley PM, Wright S, Sales J, Chianini F, Buxton D, Innes EA.** 2006. Long-term passage of tachyzoites in tissue culture can attenuate virulence of *Neospora caninum* in vivo. Parasitology **133:**421-432.
2. **King JS, McAllan B, Spielman DS, Lindsay SA, Hurkova-Hofmannova L, Hartigan A, Al-Qassab SE, Ellis JT, Slapeta J.** 2011. Extensive production of *Neospora caninum* tissue cysts in a carnivorous marsupial succumbing to experimental neosporosis. Vet Res **42:**75.

3. **Lindsay SA, Barrs VR, Child G, Beatty JA, Krockenberger MB.** 2010. Myelitis due to reactivated spinal toxoplasmosis in a cat. J Feline Med Surg **12:**818-821.

4. **Yu H, Huang B, Zhuo X, Chen X, Du A.** 2013. Evaluation of a real-time PCR assay based on the single-copy SAG1 gene for the detection of *Toxoplasma gondii*. Vet Parasitol **197:**670-673.

5. **Collantes-Fernandez E, Zaballos A, Alvarez-Garcia G, Ortega-Mora LM.** 2002. Quantitative detection of *Neospora caninum* in bovine aborted fetuses and experimentally infected mice by real-time PCR. J Clin Microbiol **40:**1194-1198.

6. **Hellemans J, Mortier G, De Paepe A, Speleman F, Vandesompele J.** 2007. qBase relative quantification framework and software for management and automated analysis of real-time quantitative PCR data. Genome Biol **8:**R19.

7. **Higgins DP, Hemsley S, Canfield PJ.** 2004. Assessment of anti-bovine IL4 and IFN gamma antibodies to label IL4 and IFN gamma in lymphocytes of the koala and brushtail possum. Vet Immunol Immunopathol **101:**153-160.

8. **Maher IE, Griffith JE, Lau Q, Reeves T, Higgins DP.** 2014. Expression profiles of the immune genes CD4, CD8beta, IFNgamma, IL-4, IL-6 and IL-10 in mitogen-stimulated koala lymphocytes (*Phascolarctos cinereus*) by qRT-PCR. PeerJ **2:**e280.

9. **Haas BJ, Papanicolaou A, Yassour M, Grabherr M, Blood PD, Bowden J, Couger MB, Eccles D, Li B, Lieber M, Macmanes MD, Ott M, Orvis J, Pochet N, Strozzi F, Weeks N, Westerman R, William T, Dewey CN, Henschel R, Leduc RD, Friedman N, Regev A.** 2013. De novo transcript sequence

reconstruction from RNA-seq using the Trinity platform for reference generation and analysis. Nat Protoc **8:**1494-1512.

10. **Robinson MD, Oshlack A.** 2010. A scaling normalization method for differential expression analysis of RNA-seq data. Genome Biol **11:**R25.

11. **Untergasser A, Nijveen H, Rao X, Bisseling T, Geurts R, Leunissen JA.** 2007. Primer3Plus, an enhanced web interface to Primer3. Nucleic Acids Res **35:**W71-74.

12. **Thornton B, Basu C.** 2011. Real-time PCR (qPCR) primer design using free online software. Biochem Mol Biol Educ **39:**145-154.

13. **Ye J, Coulouris G, Zaretskaya I, Cutcutache I, Rozen S, Madden TL.** 2012. Primer-BLAST: a tool to design target-specific primers for polymerase chain reaction. BMC Bioinformatics **13:**134.

14. **Daly KA, Mailer SL, Digby MR, Lefevre C, Thomson P, Deane E, Nicholas KR, Williamson P.** 2009. Molecular analysis of tammar (*Macropus eugenii*) mammary epithelial cells stimulated with lipopolysaccharide and lipoteichoic acid. Vet Immunol Immunopathol **129:**36-48.

15. **Mar JC, Kimura Y, Schroder K, Irvine KM, Hayashizaki Y, Suzuki H, Hume D, Quackenbush J.** 2009. Data-driven normalization strategies for high-throughput quantitative RT-PCR. BMC Bioinformatics **10:**110.

16. **Bustin SA, Benes V, Garson JA, Hellemans J, Huggett J, Kubista M, Mueller R, Nolan T, Pfaffl MW, Shipley GL, Vandesompele J, Wittwer CT.** 2009. The MIQE guidelines: minimum information for publication of quantitative real-time PCR experiments. Clin Chem **55:**611-622.

Supplementary Text S2 Histopathological changes in *Toxoplasma gondii* infected dunnarts at 7 and 14 days p.i. and *Neospora caninum* infected dunnarts at 7 and 13 days p.i.

Histopathologic lesions in *T. gondii* infected dunnarts were similar to what has been described for toxoplasmosis in other species (1) and largely consisted of nonsuppurative variably neutrophilic inflammation and necrosis in multiple tissues with the mesentery, lung, and heart being the most severely affected tissues at 14 days p.i. Tachyzoites were often only identified in IHC stained sections, were more commonly detected in areas of necrosis and generally associated with neutrophilic infiltrates. Tissue cysts were uncommon and only found in *T. gondii* infected animals at 14 days p.i.; presence of tissue cysts was confirmed using *T. gondii* BAG5 IHC. All animals had granulomatous to pyogranulomatous variably necrotizing peritonitis with intralesional tachyzoites and occasional extension of inflammatory infiltrates into body wall and subvertebral skeletal muscle. Severity of peritonitis varied from minimal to marked at 7 days p.i. and minimal to moderate at 14 days p.i. In some animals, serosal inflammation of the gastrointestinal tract extended into the subserosal connective tissue and smooth muscle. Inflammation of the gastric and intestinal muscular tunics was generally minimal to mild and more common in animals at 14 days p.i. At 7 days p.i., changes in the lungs were limited to patchy areas in which alveolar septa were mildly thickened with macrophages and occasional lymphocytes. At 14 days p.i. animals had moderate to marked interstitial pneumonia characterized by multifocal to coalescing accumulations of macrophages with fewer admixed neutrophils, lymphocytes, plasma cells and

scattered necrotic cellular debris that thickened alveolar septa and replaced air spaces. Many alveolar spaces were lined by hyperplastic type II pneumocytes and contained variable quantities and combinations of macrophages, lymphocytes, plasma cells, oedema fluid, and fibrin. Tachyzoites were identified in pulmonary epithelial cells, unidentified cells in the interstitium, and were found both free and within macrophages in alveolar spaces. At 7 days p.i., the myocardium of three of four animals contained rare minimal infiltrates of mononuclear cells and rare necrotic myofibers; in one animal a few tachyzoites were detected in association with a focus of inflammation. At 14 days p.i., a minimal to moderate multifocal nonsuppurative variably neutrophilic myocarditis and myonecrosis was present. Lesions in the heart were most pronounced in the myocardium but also involved the epicardium and endocardium. Intralesional tachyzoites were commonly found in areas of necrosis and tissue cysts were identified in three of four animals.

Histopathologic changes were consistently detected in all animals at both time points in the diaphragm, liver, and lymphoid tissues. Lesions in the diaphragm consisted of mild to moderate granulomatous myositis and myonecrosis with fibroplasia and mineralization seen at 14 days p.i. Intralesional tachyzoites were identified at 7 days p.i. in two of four animals while low numbers of tachyzoites and tissue cysts were only found in one animal at 14 days p.i. Hepatic lesions were minimal and consisted of scattered small random foci of coagulative necrosis associated with neutrophilic infiltrates at 7 days p.i. and small scattered clusters of mononuclear cells with rare admixed necrotic cellular debris at 14 days p.i. Tachyzoites were only rarely detected in the liver at 7 days p.i. in areas of necrosis and *T. gondii* antigen was identified by IHC in

sinusoidal Kupffer cells. At 7 days p.i., the spleen, mesenteric and thoracic lymph nodes had moderate to marked lymphoid hyperplasia characterized by large reactive lymphoid follicles with prominent germinal centers. Some lymph nodes also had mild to moderate sinusoidal histiocytosis. Additional findings at 14 days p.i. included prominent central lymphocytolysis in the majority of lymphoid follicles, minimal to moderate granulomatous lymphadenitis involving mesenteric and less commonly thoracic lymph nodes, and variable amounts of blood and oedema fluid within mesenteric lymph node sinuses. Similar lymphoid hyperplasia and inflammation was observed in submandibular and sublumbar lymph nodes available for evaluation. Tachyzoites were detected in areas of splenic and lymph node capsular inflammation and in the mesenteric lymph node sinuses of one animal at 7 days p.i. IHC staining revealed *T. gondii* antigen within rare cells in the spleen at 14 days p.i. in one animal and in multiple thoracic and mesenteric lymph nodes at both time points.

Additional light microscopic changes associated with *T. gondii* infection were more variable and included mild to moderate granulomatous to pyogranulomatous rarely necrotizing cystitis generally limited to serosal and smooth muscle layers (one of four animals at 7 days p.i. and three of four animals at 14 days p.i.), minimal necrotizing adrenalitis (three of four animals at 14 days p.i.), mild to moderate nonsuppurative to pyogranulomatous and necrotizing cholecystitis (two of four animals at 7 and 14 days p.i.), minimal to mild pancreatitis that varied from focal and nonsuppurative at 7 days p.i. (one of four animals) to granulomatous and necrotizing at 14 days p.i. (all animals), minimal to mild nonsuppurative glossitis (one animal at 7 days p.i. and four animals at 14 days p.i.), focal minimal lymphoplasmacytic meningitis (one of four animals at 14

days p.i.), moderate suppurative ureteritis (one of four animals at 7 days p.i.), and mild focal granulomatous and necrotizing prostatitis limited to the serosa and subserosal smooth muscle (one animal at 14 days p.i.). Tachyzoites were occasionally identified in association with lesions in the smooth muscle layers of the stomach (one of four animals at 14 days p.i.), jejunum (one of four animals at 14 days p.i.), colon (all animals at 14 days p.i.), gall bladder (one of four animals at 7 and 14 days p.i.), and urinary bladder (one of four animals at 14 days p.i.). Tachyzoites were also identified in subvertebral skeletal muscle (three of four animals at 7 days p.i. and all animals at 14 days p.i.), forelimb skeletal muscle (one animal at 14 days p.i.), pancreas (three of four animals at 14 days p.i.), and tongue (one animal at 7 days p.i.). Small numbers of tissue cysts were detected at 14 days p.i. in the diaphragm (one of four animals), perivertebral skeletal muscle (one of four animals), and urinary bladder (one of four animals), and a single cyst was identified in the kidney of one animal.

Sections of spinal cord, trachea, esophagus, elbow joint, bone, bone marrow, external ear, skin, brain, elbow joint, peripheral nerve, thyroid gland, pituitary gland (not consistently examined), thymus, testicle, and epididymis were histologically normal in *T. gondii* infected animals at 7 and 14 days p.i. or contained changes similar to uninfected control animals.

In *N. caninum* infected animals, predominant lesions in visceral tissues were necrosis followed by inflammation that varied from granulomatous to pyogranulomous with muscle, liver, lung, and pancreas most severely affected. Peritonitis was also a common feature and was usually most pronounced in the mesometrium, in the vicinity of genitourinary structures, and the gastroduodenal junction and pancreas. Overall,

histopathologic lesions were generally more widespread and severe in *N. caninum* infected animals than *T. gondii* infected animals at similar time points. Replicating tachyzoites were commonly identified both in association with lesions as well as in the absence of an appreciable inflammatory response and tissue cysts were confirmed by *T. gondii* BAG5 IHC (which cross reacts with *N. caninum* bradyzoites and cysts) in a wide range of tissues at 13 days p.i. but not at 7 days p.i.

Consistent with previous descriptions of neosporosis in dunnarts (2), some of the most striking lesions were in muscle and involved cardiac, striated, and smooth muscle. Heart lesions were seen in all animals and consisted of minimal focal to multifocal nonsuppurative myocarditis with minimal to mild myonecrosis at 7 days p.i. and moderate multifocal to coalescing nonsuppurative to pyogranulomatous myocarditis with moderate to severe myonecrosis at 13 days p.i. Intralesional tachyzoites were common and small numbers of tissue cysts were seen in all animals at 13 days p.i. Of sections of skeletal muscle evaluated, the diaphragm was most severely affected followed by subvertebral skeletal muscle. The diaphragm in all animals had multifocal to coalescing granulomatous to pyogranulomatous myositis and myonecrosis with intralesional tachyzoites that varied from mild to marked at 7 days p.i. to severe at 13 days p.i. Similar changes were consistently identified in the subvertebral musculature and were minimal to moderate at 7 days p.i. and moderate to severe at 13 days p.i. Tissue cysts were detected in the diaphragm of all animals at 13 days p.i. and in subvertebral muscle in three of four animals. In the tongue, minimal to moderate lymphoplasmacytic glossitis and minimal to mild myonecrosis was seen in all animals at 7 days p.i. and moderate to severe lymphoplasmacytic to granulomatous glossitis with moderate to severe

myonecrosis was evident in all animals at 13 days p.i. Intralesional tachyzoites were identified in two of four animals at 7 days p.i. and in all animals at 13 days p.i. Tissue cysts were seen in the tongue of three animals at 13 days p.i. Myositis and myonecrosis with intralesional tachyzoites were also seen in sections of periocular and forelimb skeletal muscle. Tissue cysts were identified in periocular muscle of two of four animals, four of four animals in forelimb skeletal muscle at 13 days p.i. Similar to *T. gondii* infected dunnarts, inflammatory infiltrates frequently extended from the serosal surface into muscular tunics of abdominal viscera. The urinary bladder and gall bladder were consistently and most severely affected. A multifocal to rarely transmural granulomatous to necrosuppurative cystitis was seen in all animals that varied from mild to moderate at 7 days p.i. and mild to severe at 13 days p.i. Intralesional tachyzoites were common and replicating tachyzoites were also identified in the absence of a host response. Many tissue cysts were seen in the urinary bladder smooth muscle at 13 days p.i. The gall bladder had multifocal to transmural granulomatous to pyogranulomatous variably necrotizing cholecystitits with intralesional tachyzoites that was severe at 7 days p.i. and mild to severe at 13 days p.i. Histopathologic lesions in gastrointestinal smooth muscle were less consistent. Minimal to rarely moderate inflammation and necrosis associated with tachyzoites were found in smooth muscle of the stomach (three of four animals at 7 days p.i. and all animals at 13 days p.i.), duodenum (two of four animals at 7 and 13 days p.i.), jejunum (three of four animals at 7 days p.i. and all animals at 13 days p.i.), and colon (two of four animals at 7 days p.i. and three of four animals at 13 days p.i.). In the stomach, replicating tachyzoites were identified in parietal and chief cells and mucosal epithelial cells at 13 days p.i. Granulomatous to necrotizing esophagitis with

occasional intralesional tachyzoites predominately involved smooth muscle and varied from minimal to mild at 7 days p.i. (two of three animals) and minimal to marked at 13 days p.i. (three of four animals). Lesions in the uterus were characterized by granulomatous to pyogranulomatous and necrotizing myometritis with intralesional zoites that varied from mild to moderate at 7 days p.i. (two of three animals) and was moderate and included endometritis at 13 days p.i. (2 of 3 animals). Lesions in the oviduct and ovary included a marked pyogranulomatous and necrotizing salpingitis involving smooth muscle with intralesional zoites (one of three animals at 7 and 14 days p.i.) and a moderate to marked granulomatous and necrotizing oophoritis at 13 days p.i. (two of three animals) with intralesional zoites identified in one animal. Smooth muscle of the vagina and cervix also contained mild to moderate granulomatous and necrotizing inflammation with occasional intralesional zoites at 13 days p.i. (two of three animals). Similar mild smooth muscle lesions were in the prostate and penis of one animal at 13 days p.i.

Hepatic and pulmonary lesions were consistently identified in all animals. At 7 days p.i., the liver contained multifocal random foci of acute necrosis consisting of admixed accumulations of fibrin, neutrophils, and necrotic cellular debris. These lesions correlated grossly with the red foci of discolored parenchyma noted at necropsy. Intralesional tachyzoites were occasionally detected in association with necrotic foci. At 14 days p.i., extensive multifocal to coalescing hepatic necrosis with mild to moderate accumulations of mononuclear cells, neutrophils, fibrin, and hemorrhage was seen in all animals. Tachyzoites were found replicating within hepatocytes and biliary epithelial cells and were also found free in and within Kupffer cells in the sinusoids. Lesions in the

lungs at 7 days p.i. were characterized by minimal to mild thickening of alveolar septa with small numbers of macrophages and neutrophils, edema fluid, and occasional accumulations of fibrin. At 13 days p.i., all animals had a moderate to severe interstitial pneumonia characterized by diffuse expansion of alveolar septa with many macrophages and neutrophils, edema fluid, and fibrin. Alveolar histiocytosis, fibrin exudation and necrotic debris within alveoli, type II pneumocyte hyperplasia, hyaline membrane formation, pulmonary edema, and atelectasis were also evident. Tachyzoites were identified in alveolar septa, pneumocytes, and within alveoli both free and within macrophages.

The pancreas had nonsuppurative to pyogranulomatous and necrotizing pancreatitis that varied from focal and minimal to multifocal and mild at 7 days p.i. (three of four animals) and was multifocal to coalescing and minimal to marked at 13 days p.i. Intralesional tachyzoites were numerous in areas of necrosis and were also found replicating within acinar epithelial cells. Lesions in the brain at 7 days p.i were only identified in one animal and included minimal multifocal nonsuppurative to pyogranulomatous meningitis and minimal multifocal necrotizing encephalitis; intralesional tachyzoites were not identified. The pituitary gland of the same animal had a small focus of acute necrosis in the pars nervosa associated with intralesional tachyzoties. At 14 days p.i., minimal to mild nonsuppurative meningitis, nonsuppurative to necrotizing encephalitis with intralesional tachyzoites, and one to several tissue cysts were identified in all animals. Lesions in the spinal cord were seen in three of four animals at 13 days p.i. and consisted of rare minimal foci of necrosis and gliosis, minimal multifocal lymphoplasmacytic meningitis, and minimal to mild nonsuppurative

spinal ganglioneuritis. Rare intralesional tachyzoites were detected in association with these lesions and tissue cysts were identified in two animals.

With regards to lymphoid tissue, lymphoid hyperplasia was rarely apparent in dunnarts with neosporosis and when identified was generally minimal to mild. Multifocal granulomatous to pyogranulomatous and necrotizing splenitis was evident in all animals and varied from minimal to marked at 7 days p.i. and mild to marked at 13 days p.i. Intralesional tachyzoites were identified in two animals at 7 days p.i. and in all animals at 13 days p.i. At 13 days p.i., the spleen had extramedullary hematopoiesis beyond baseline levels characterized by a preponderance of myeloid precursors and increased numbers of megakaryocytes. The mesenteric lymph nodes had mild to marked granulomatous to pyogranulomatous variably necrotizing lymphadenitis (three of three animals at 7 days p.i., three of four animals at 13 days p.i.). The thoracic lymph node had similar marked lymphadenitis (one of one animal at 7 days p.i., three of three animals at 13 days p.i.) as did other lymph nodes when available for evaluation.

Additional histopathologic lesions associated with *N. caninum* infection included minimal to mild nonsuppurative and necrotizing sialoadenitis with intralesional tachyzoites and replicating tachyzoites in acinar epithelial cells (three of four at 7 days p.i. and 13 days p.i.), necrotizing adrenalitis with intralesional tachyzoites (minimal in one of three animals at 7 days p.i., moderate in three of four animals at 13 days p.i.), moderate pyogranulomatous and necrotizing ureteritis (one of four animals at 7 days p.i. and one of three animals at 13 days p.i.), pyogranulomatous pyelonephritis (one of four animals at 13 days p.i.), and mild focal to multifocal granulomatous and necrotizing thyroiditis with intralesional tachyzoites and rare replicating tachyzoites in follicular

epithelial cells (two of two animals at 13 days p.i.), focal granulomatous epididymitis (one of one animal at 13 days p.i.), and marked atrophy of tail adipose tissue (four of four animals at 13 days p.i.). In addition to the tissues listed above, small numbers of tachyzoites were also identified in the bone marrow in megakaryocytes and myeloid precursors in *N. caninum* infected animals at 13 days p.i. Tissue cysts were identified at 13 days p.i. in the colonic muscularis (one animal), pancreas (one animal), cranial nerve ganglion (one animal), adrenal gland (two animals), penis musculature (one animal), and prostate smooth muscle (one animal). Sections of spinal cord, peripheral nerve, trachea, thyroid gland, thymus, testicle, ovary, and elbow joint in dunnarts at 7 days p.i. and the thymus of dunnarts at 13 days p.i. were histologically normal. One animal at 13 days p.i. had a focal granulomatous epididymitis and another had a mild nonsuppurative synovitis of the shoulder joint; however, intralesional tachyzoites were not identified and the association of these lesions to parasite infection could not be established.

References

1. **Dubey JP.** 2010. Toxoplasmosis of animals and humans, 2nd ed. CRC Press, Boca Raton.
2. **King JS, McAllan B, Spielman DS, Lindsay SA, Hurkova-Hofmannova L, Hartigan A, Al-Qassab SE, Ellis JT, Slapeta J.** 2011. Extensive production of *Neospora caninum* tissue cysts in a carnivorous marsupial succumbing to experimental neosporosis. Vet Res **42:**75.

Figure S1

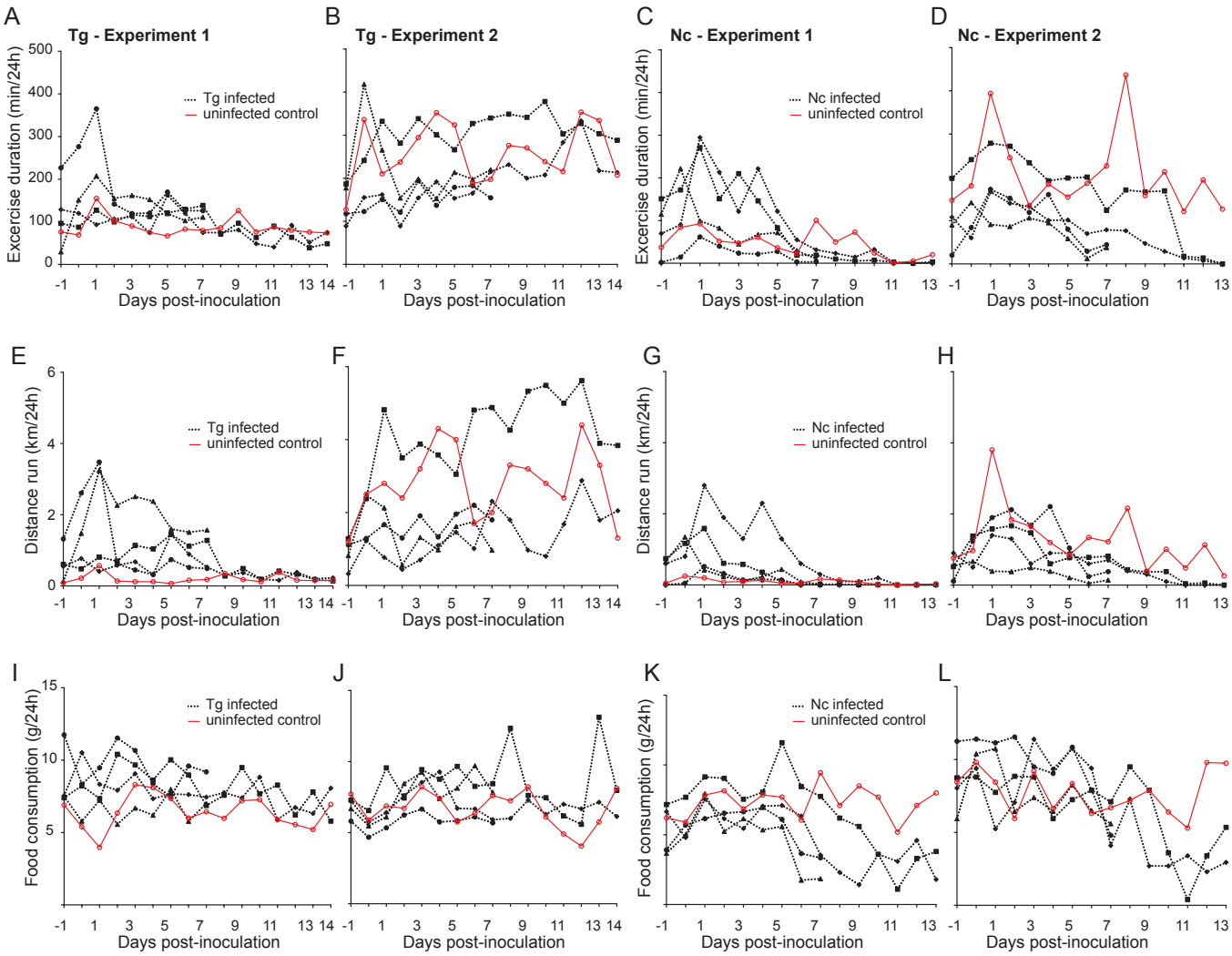
A
Tg - Experiment 1
B
Tg - Experiment 2
C
Nc - Experiment 1
D
Nc - Experiment 2
Excercise duration (min/24h)
Tg infected
uninfected control
Nc infected
uninfected control
Days post-inoculation
E
F
G
H
Distance run (km/24h)
I
J
K
L
Food consumption (g/24h)

Supplementary Figure 1: Daily activity and food consumption of fat-tailed dunnarts (*Sminthopsis crassicaudata*) during *Neospora caninum* and *Toxoplasma gondii* infection. Data shown are representative of two independent *T. gondii* experiments (Tg1: A, E, I; Tg2: B, F, J) and two independent *N. caninum* experiments (Nc1: C, G, K; Nc2: D, H, L). Activity and food consumption of all experimental animals was individually monitored and is presented as a daily sum. Daily activity was measured on an exercise wheel equipped with a wheel odometer that translated the number of revolutions in 24 hours into distance in kilometers (C, D, I, J) and time spent in the wheel (A, B, G, H). Food consumption reflects the total grams of food consumed in 24 hours (E, F, K, L). Uninfected control animals are designated by a red line connecting data points.

TABLE S1 Summary of parasite infection experiments in the fat-tailed dunnart (*Sminthopsis crassicaudata*)

Experiment	Parasite	Identification	Sex	Euthanasia (days p.i.)	MAT/cELISA (%I)[a]
Tg1	*T. gondii*	Tg1A	M	7	Neg.
		Tg1B	M	7	Neg.
		Tg1C	M	14	Pos.
		Tg1D	M	14	Pos.[c]
		Tg1-control[b]	F	14	Neg.
Tg2	*T. gondii*	Tg2A	M	7	Neg.
		Tg2B	M	7	Neg.
		Tg2C	M	14	Pos.
		Tg2D	M	14	Pos.[c]
		Tg2-control[b]	F	14	NT
Nc1	*N. caninum*	Nc1A	F	7	Neg. (7%)
		Nc1B	M	7	Neg. (24%)
		Nc1C	F	13[d]	Pos. (39%)
		Nc1D	M	13[d]	Pos. (59%)
		Nc1-control[b]	M	13	Neg. (13%)
Nc2	*N. caninum*	Nc2A	F	7	Neg. (3%)
		Nc2B	F	7	Neg. (16%)
		Nc2C	F	13[d]	Pos. (62%)
		Nc2D	F	13[d]	Neg. (12%)
		Nc2-control[b]	F	13	Neg. (13%)

[a] cELISA and MAT were used to detect *N. caninum* and *T. gondii* antibodies, respectively

[b] negative control animal

[c] weak positive MAT reaction

[d] animal euthanized due to clinical neosporosis for animal welfare reasons

Note. cELISA, competitive enzyme-linked immunosorbent assay; MAT, modified agglutination test; NT, not tested; p.i., postinfection

TABLE S2 Primers used in this study

Gene	Primers (5'-3')	T (°C) Annealing	Amplicon size (bp)	Reference
Nc5 *(N. caninum)*	F: ACTGGAGGCACGCTGAACAC R: AACAATGCTTCGCAAGAGGAA	60	76	E. Collantes-Fernandez et al., 2002(1)
SAG1 *(T. gondii)*	F: CTGATGTCGTTCTTGCGATGTGGC R: GTGAAGTGGTTCTCCGTCGGTGT	60	128	Yu et al., 2013(2)
GAPDH*	F: AACTTTGGCATTGTGGAAGGA R: GTGGAAGCAGGGATGATGTT	57	134	Maher et al., 2014(3)
28S*	F: CGATGTCGGCTCTTCCTATC R: TCCTCAGCCAAGCACATACA	60	205	Daly et al., 2009(4)
TNF-α	F:TGATACCTGCCTCTGGACTTTAC R:GCTTCTCTTGTTGCCTTCTGG	60	178	This study
IL-6	F:AAATCCAGCATCGGGCAGTG R:AAATCTTGTTCTTCAGGTCAGTAGC	57	91	This study
IL-4	F:ACTGTTGCCACTTTGTTGATAGA R:GCTTCGGCAGTTTCTTCTCT	60	125	This study
IFN-γ	F:TGGAGCATATCAAAGAGGACAT R:GGGTGAGAAGTTACGGAAGAC	60	161	This study
IL-17A	F: GTGCCGTCATTCAGGTTGC R: GGTGACACAGGTACATCCTACAG	60	166	This study

Note. An asterisk denotes primers used as reference genes

References

1. **Collantes-Fernandez E, Zaballos A, Alvarez-Garcia G, Ortega-Mora LM.** 2002. Quantitative detection of *Neospora caninum* in bovine aborted fetuses and experimentally infected mice by real-time PCR. J Clin Microbiol **40:**1194-1198.
2. **Yu H, Huang B, Zhuo X, Chen X, Du A.** 2013. Evaluation of a real-time PCR assay based on the single-copy SAG1 gene for the detection of *Toxoplasma gondii*. Vet Parasitol **197:**670-673.
3. **Maher IE, Griffith JE, Lau Q, Reeves T, Higgins DP.** 2014. Expression profiles of the immune genes CD4, CD8beta, IFNgamma, IL-4, IL-6 and IL-10 in mitogen-stimulated koala lymphocytes (*Phascolarctos cinereus*) by qRT-PCR. PeerJ **2:**e280.
4. **Daly KA, Mailer SL, Digby MR, Lefevre C, Thomson P, Deane E, Nicholas KR, Williamson P.** 2009. Molecular analysis of tammar (*Macropus eugenii*) mammary epithelial cells stimulated with lipopolysaccharide and lipoteichoic acid. Vet Immunol Immunopathol **129:**36-48.

TABLE S3 Optimization values for qPCR assays used in this study

Gene	Efficiency	Conc (nM)	Linear dynamic range (orders of magnitude)	LOQ (copies/ qPCR reaction)	Cq at LOQ	LOD (copies/ qPCR reaction)	r^2 calibration curve	Slope	y-intercept
Nc5	0.991	1000	7	6	31	<1	1.000	-3.343	33.733
SAG1	0.980	400	8	18	35	2	0.997	-3.371	38.865
GAPDH	0.974	500	8	8	36	1	0.998	-3.385	41.681
28S	0.993	250	9	4	35	<1	0.999	-3.340	38.582
TNF-α	0.985	500	8	461	35	30	0.997	-3.358	41.198
IL-6	0.985	500	8	722	35	72	0.996	-3.359	43.725
IL-4	0.987	250	9	3580	37	358	0.996	-3.354	46.176
IFN-γ	0.990	500	9	37	36	6	0.999	-3.346	37.754
IL-17A	0.983	500	9	2	36	2	0.998	-3.363	38.423

Notes. Conc, primer concentration (nM); LOQ, limit of quantification; LOD, limit of detection

TABLE S4 Summary of histopathology lesion grading scores for inflammation, necrosis, and parasite life stage in *Neospora caninum* and *Toxoplasma gondii* infected fat-tailed dunnarts (*Sminthopsis crassicaudata*)

	Results[a]				
		N. caninum days postinfection		*T. gondii* days postinfection	
Tissue and histopathology	Control	7	13	7	14
Brain					
Inflammation	0,0,0,0	0,0,1,0	1,1,2,1	0,0,0,0	0,1,0,0
Necrosis	0,0,0,0	0,0,1,0	1,1,2,1	0,0,0,0	0,0,0,0
Parasite life stage	0,0,0,0	0,0,0,0	1,1,3,3	0,0,0,0	0,1,0,0
Tongue					
Inflammation	0,0,1,0	1,2,3,1	3,3,4,3	1,2,0,1	1,1,2,2
Necrosis	0,0,0,0	1,1,2,1	3,3,4,3	1,2,0,1	1,0,1,1
Parasite life stage	0,0,0,0	0,1,1,0	1,3,1,1	0,1,0,0	0,0,0,0
Lung					
Inflammation	0,1,0,1	2,3,2,3	4,3,4,4	3,2,2,2	4,4,3,3
Necrosis	0,0,0,0	1,2,2,2	4,4,4,4	1,2,2,2	2,3,3,2
Parasite life stage	0,0,0,0	1,1,1,1	1,1,1,1	0,0,0,0	0,1,1,1
Heart					
Inflammation	0,1,0,0	1,1,1,1	3,3,3,3	1,2,1,1	2,3,2,1
Necrosis	0,0,0,0	1,2,2,1	4,4,4,3	1,1,1,0	2,3,3,1
Parasite life stage	0,0,0,0	1,1,1,1	3,3,3,1	0,1,0,0	1,3,3,1
Liver					
Inflammation	0,0,0,1	3,3,3,2	4,2,4,3	1,1,1,2	1,1,1,1
Necrosis	0,0,0,0	3,3,3,3	4,2,4,4	1,1,1,2	0,0,1,1
Parasite life stage	0,0,0,0	1,1,1,1	1,1,1,1	1,1,0,1	0,0,0,0
Spleen					
Inflammation	0,0,0,0	3,1,4,2	3,2,4,2	1,0,0,3	1,1,1,2
Necrosis	0,0,0,0	2,2,3,1	3,3,3,1	0,0,0,3	0,0,0,0
Parasite life stage	0,0,0,0	1,0,1,0	1,1,1,1	1,0,0,1	1,0,0,0

[a]For the evaluated sectional area of each tissue, the extent of inflammation and necrosis were semiquantitatively ranked with scores ranging from no lesion present (score = 0) to minimal (<5% affected; score = 1), mild (5-10% affected; score = 2), moderate (11-30% affected; score = 3), or severe (>30% affected; score = 4). To evaluate for the presence of different parasite life stages, scoring ranged from none present (score = 0) to tachyzoites only (score = 1), tissue cysts only (score = 2), or tachyzoites and tissue cysts (score = 3). The presence of tissue cysts was confirmed using bradyzoite specific BAG5 IHC.

TABLE S5 Summary of tissue parasite load (no. parasites/100ng DNA) in fat-tailed dunnarts (*Sminthopsis crassicaudata*) infected with *Neospora caninum* and *Toxoplasma gondii* at 1 and 2 weeks postinfection

	Parasite			
	N. caninum		*T. gondii*	
Tissue	7 days p.i.	13 days p.i.	7 days p.i.	14 days p.i.
Brain	9.14 (5.71 - 4.19 × 10^1)	1.36 × 10^3 (6.01 × 10^2 - 1.87 × 10^3)	0.00 (0.00 - 0.00)	0.00 (0.00 - 1.88 ×10^2)
Tongue	3.38 × 10^2 (7.87 × 10^1 - 7.95 × 10^2)	1.71 × 10^4 (1.18 × 10^4 - 2.58 × 10^4)	1.42 × 10^1 (0.00 - 1.10 × 10^2)	2.65 × 10^1 (0.00 - 6.63 × 10^1)
Lung	1.84 × 10^3 (7.91 × 10^2 - 4.17 × 10^3)	2.57 × 10^4 (1.76 × 10^4 - 3.52 × 10^4)	8.84 × 10^1 (4.74 × 10^1 - 1.53 × 10^2)	4.18 × 10^2 (1.01 × 10^2 - 6.33 × 10^2)
Heart	5.57 × 10^3 (2.08 × 10^3 - 1.09 × 10^4)	1.90 × 10^5 (8.24 × 10^4 - 3.02 × 10^5)	3.81 × 10^1 (2.86 × 10^1 - 8.68 × 10^1)	2.45 × 10^3 (4.46 × 10^2 - 5.70 × 10^3)
Liver	1.89 × 10^3 (6.04 × 10^2 - 8.30 × 10^3)	2.54 × 10^4 (7.74 × 10^3 - 3.22 × 10^4)	2.35 × 10^2 (2.93 × 10^1 - 4.60 × 10^2)	0.00 (0.00 - 1.54 × 10^1)
Spleen	7.93 × 10^1 (3.27 × 10^1 - 4.27 × 10^2)	2.24 × 10^3 (8.88 × 10^2 - 5.30 × 10^3)	1.00 × 10^1 (0.00 - 3.05 × 10^1)	2.13 × 10^1 (3.21 - 3.24 × 10^1)

Note. Parasite numbers represent group median value (interquartile range) based on 4 biological replicates. Data shown are representative of two independent *T. gondii* experiments and two independent *N. caninum* experiments. p.i., postinfection.

TABLE S6 Summary of cytokine mRNA expression in the spleen of fat-tailed dunnarts (*Sminthopsis crassicaudata*) at one and two weeks postinfection with *Toxoplasma gondii* and *Neospora caninum*

	Fold change				
Group	IFN-γ expression	TNF-α expression	IL-4 expression	IL-6 expression	IL-17A expression
Control	1.182 (0.6193 - 1.504)	0.7927 (0.584-0.88)	0.9841 (0.881 – 1.158)	1.068 (0.5807 – 1.762)	1.546 (0.3642 – 3.353 0
N. caninum, 7 days p.i.	40.16 (29.94 - 44.06)	2.678 (2.127-4.723)	0.6851 (0.6685 – 1.974)	0.8932 (0.6322 – 1.219)	5.736 (1.025 – 21.29)
T. gondii, 7 days p.i.	49.27 (37.6 - 73.14)	2.532 (1.657 - 4.926)	1.35 (0.9337 – 1.66)	1.333 (0.7734 – 4.044)	0.4604 (0.0504 – 0.9412)
N. caninum, 13 days p.i.	117.5 (28.74 - 159.9)	3.072 (1.878 - 4.05)	2.768 (2.003 – 3.612)	0.8932 (0.6322 – 1.219)	2.027 (0.7897 – 15.71)
T. gondii, 14 days p.i.	283.7 (235 - 366.5)	6.206 (3.994 – 7.63)	2.232 (1.01 – 3.012)	1.323 (1.148 – 1.773)	0.4291 (0.0244 – 1.424)

Note. Data are group median values (interquartile ranges) based on four biological replicates. Data shown are representative of two independent *T. gondii* experiments and two independent *N. caninum* experiments. Control, uninfected dunnarts; p.i., postinfection.